Three-dimensional constraint theory：Bridge the gap from laboratory material tests to fatigue fracture of engineering structures

Wanlin Guo, Peishi Yu and Zhenbo Yu

School of Frontier Science, Nanjing University of Aeronautics and Astronautics, No.29 of Yudao Street, Nanjing 210016, China

Keyword: Three-dimensional fracture, Out-of-plane constraint, Fracture criterion, Fatigue life.

Abstract. The methods to assess structural strength and fracture theories have been developed for several decades, and have been successful for many specific engineering applications. Here we report the recent progresses from two-dimensional (2D) to three-dimensional (3D) fracture theories based on two- and three-parameter descriptions, such as K-T_z, J-T_z and K-T-T_z, J-Q_T-T_z, and their applications in bridging the gap from academic researches and material tests in laboratories to practical engineering structures. Here, T and Q are parameters for in-plane constraints, while T_z is the out-of-plane constraint factor as a ratio of the out-of-plane stress to the sum of in-plane stresses. The following critical issues will be addressed: 1) From 2D fracture mechanics to 3D fracture mechanics; 2) From tensile to mixed mode loadings; 3) From static/toughness to fatigue/durability; 4) From ambient to complex environments; 5) From empirical design to predictive design; 6) From design to fatigue life assessment.

1. Introduction

The current damage tolerance design of structures is based on the fracture mechanics theory. The linear elastic fracture mechanics was founded based on the theory of the stress intensity factor (SIF, K) introduced by Irwin [1] in 1948. Subsequently, Williams proposed a two-parameter K-T approach for the isotropic linear elastic materials in 1957 [2].

$$\sigma_{ij} = \frac{K}{\sqrt{2\pi r}} f_{ij}(\theta) + T\delta_{1i}\delta_{1j} \tag{1}$$

In 1968，Rice proposed the conception of J-integral [3]; Hutchinson, Rice and Rosengren obtained the asymptotic crack-tip solution (HRR solution) for power hardening materials [4,5]. The HRR solution and Rice's J-integral were obtained under the frame of deformation theory of plasticity, it was shown by large amount of numerical and experimental researches that the HRR solutions coincide very well with the finite element results based on flow theory and J dominates the crack tip field effectively in plane stress state, but in the plane strain state the J

dominated region is much smaller and dependent on loading type and geometrical configurations. In 1989, a two term higher order J-A_2 solution for power hardening materials was developed by Li and Wang [6]. In the early of 1990s, Al-Ani AM and Hancock proposed a similar *J*-*T* theory [7]; Shih *et al*. found by systematic numerical analyses that the second term in the higher order solution can be approximated with a constant, thus proposed the widely used *J*-*Q* description [8,9]

$$\frac{\sigma_{ij}}{\sigma_0} = \left(\frac{J}{\alpha \sigma_0 \varepsilon_0 I_n r} \right)^{\frac{1}{n+1}} \tilde{\sigma}_{ij}(\theta, n) + \delta_{ij} Q . \tag{2}$$

Subsequently, higher order solutions up to four or five terms based on two-dimensional (2D) analyses were obtained by Xia, Wang and Shih [10] and Chao, Yang and Sutton [11], and it was shown that three or four terms expansion can match the finite element results of the in-plane stresses very well. In many situations, the simple two term *K*-*T* description of (1.1) or the *J*-*Q* description of (1.4) can provide basic predication of the influence of in-plane geometry and loading constraints on the crack-tip fields. So they are widely applied in fracture analysis to consider in-plane constraints. The *J*-*T* theory can be considered as a simplification of the *J*-*Q* description in the existence of a *K* dominated region.

However, a planar stress state in finite thickness plates can only be obtained when the plates transmit in-plane uniform stresses as show by Fig. 1(a). Even in a plate subjected to in-plane loading, out-of-plane stress constraints will raise in the interior of the plate where the stress gradient exists at locations of stress concentration or near crack-tips, Fig. 1 (b) and (c). Generally, significant out-of-plane stress constraints can be found in regions with large in-plane stress gradient.

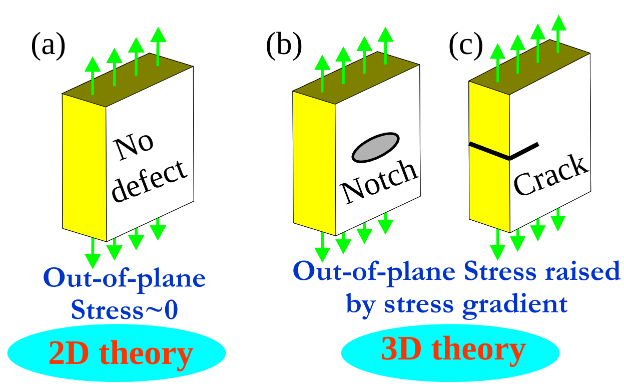

Fig. 1. Finite thickness plates under in-plane loading.

To evaluate the influence of the out-of-plane stress constraint on the crack-tip fields, the first author has introduced a so called out-of-plane stress constraint factor T_z

$$T_z = \frac{\sigma_{33}}{\sigma_{11} + \sigma_{22}}, \tag{3}$$

where the subscripts 1, 2 and 3 stand for x, y and z or r, θ and z, respectively, with z axis along the crack front line. In the plane stress state, T_z=0. In the plane strain state, T_z equals to Poisson's ratio v in elasticity and 0.5 in incompressible pure plastic media, and may change from v to 0.5 in elastic-plastic materials. In the vicinity of a crack in finite bodies, T_z generally ranges from 0 to 0.5. The HRR solution has been extended by Guo from a two-dimensional solution with T_z=0 for plane stress or T_z=0.5 for plane strain to a J-T_z solution covering the whole range of T_z from 0 to 0.5[13-15].

$$\begin{aligned} \sigma_{ij} &= \left[\frac{J}{\alpha\varepsilon_0\sigma_0 I(n,Tz) r}\right]^{\lambda(n,Tz)} \tilde{\sigma}_{ij}(\theta,Tz), \\ \varepsilon_{ij} &= \frac{3}{2}\alpha\left[\frac{J}{\alpha\varepsilon_0\sigma_0 I(n,Tz) r}\right]^{n-\lambda(n,Tz)} \tilde{\varepsilon}_{ij}(\theta,Tz). \end{aligned} \tag{4}$$

Where, the singularity exponent λ, the angular distribution and the amplitude are function of T_z.[12,13,14]

2. Three-parameter decription of the crack-tip field

Considering out-of-plane constraint, the 3D elastic and elastic-plastic stress field can be described completly by three-parameter model K-T-T_z and J-Q-T_z, which were firstly proposed by Guo[15,16,17,18].
The elastic stress field expression is

$$\begin{aligned} \sigma_{ij} &= \frac{K}{\sqrt{2\pi r}} f_{ij}(\theta) + T\delta_{1i}\delta_{1j} \\ \sigma_{33} &= T_z(\sigma_{11} + \sigma_{22}) \end{aligned}, \tag{5}$$

where

$$f_{11}(\theta) = \frac{1}{4}\left(5\cos\left(\frac{\theta}{2}\right) - \cos\left(\frac{3\theta}{2}\right)\right),\ f_{22}(\theta) = \frac{1}{4}\left(3\cos\left(\frac{\theta}{2}\right) + \cos\left(\frac{3\theta}{2}\right)\right),$$

$$f_{12}(\theta) = \frac{1}{4}\left(\sin\left(\frac{\theta}{2}\right) + \sin\left(\frac{3\theta}{2}\right)\right),\ f_{13}(\theta) = f_{23}(\theta) = 0.$$

The stress field in elastic-plastic condition can be expressed as follows

$$\frac{\sigma_{ij}}{\sigma_0}=\left(\frac{J}{\alpha\sigma_0\varepsilon_0 I\left(n,T_z\right)r}\right)^{\frac{1}{n+1}}\tilde{\sigma}_{ij}\left(\theta,n,T_z\right)+Q_{Tij}\delta_{ij}\,, \tag{6}$$

where

$$Q_{Tij}=Q+\frac{\sigma_{ij}\big|_{HRR}-\sigma_{ij}\big|_{J-T_z}}{\sigma_0}, \quad (\theta=0\,°\text{and } r=2J/\sigma 0). \tag{7}$$

Subsequently, the K-T-T_z and J-Q-T_z description of elastic and ealstic-plastic stress field at the border of various typical cracks have been obtained by 3D finite element calculations[19,20,21,22]. Parts of the stress components of K-T-T_z and J-Q-T_z description are shown in Fig. 2.[18,23] Obviously the formulae are well coincident with the numerial solution.

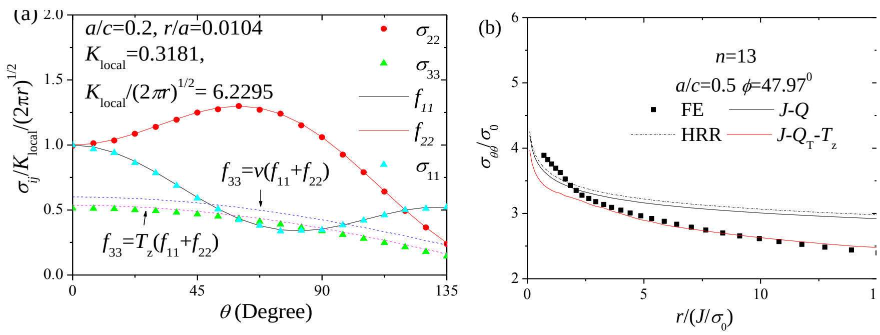

Fig. 2. (a) The elastic stress components of semi-elliptical surface crack front line at ϕ=45.14°; (b) The description of elastic-plastic stress parameters $\sigma_{\theta\theta}/\sigma_0$ of semi-elliptical surface crack front line.

A set of empirical formulae of T_z for different types of cracks are obtained by fitting the detailed numerical results. [18,19,20,21,22,24,25]

3. 3D Fracture criterions

The traditional fracture toughness parameters (K_C, J_C) are strongly dependent on the thicknesses. So a series of tests on different element thickness specimens must be carried out to obtain the whole range of fracture toughness parameters. Many scholars[26,27,28,29,30] have paid much efforts on researching the variations on fracture toughness with thicknesses on specimens.

For elastic fracture problems, Guo[31,32] proposed a 3D fracture toughness parameter K_{zc}, which was independent on specimens' thicknesses and founded a 3D fracture criterion. The 3D elastic fracture criterion can be expressed as follows

$$K_{\mathrm{IZ}} = K_{\mathrm{ZC}} = K_{\mathrm{C}}\sqrt{f\left(T_z\right)} = K_{\mathrm{C}}\sqrt{\frac{2\left[1-v-4vT_z+2T_z^2\right]}{\left(1-2T_z\right)^2}}\,, \tag{8}$$

where K_C is the plane strain fracture toughness.

The two- and three- dimensional fracture toughness parameters K_C and K_{ZC} are shown in Fig. 3 a, which reveal that the 3D fracture toughness is independent on thicknesses.

For elastic-plastic fracture problems, the J-integral criterion was applied as follows[33]

$$J_{\mathrm{Z}} = J_{\mathrm{ZC}} = J_{\mathrm{C}}\,\frac{2E\left[1-v-4vT_z+2T_z^2\right]}{\left(1-2T_z\right)^2\left(1-v^2\right)}\,, \tag{9}$$

where J_C is the planar fracture toughness.

The two- and three- dimensional fracture toughness parameters J_C and J_{ZC} are shown in Fig. 3 (b). It can be found that the 3D fracture toughness is independent on thicknesses.

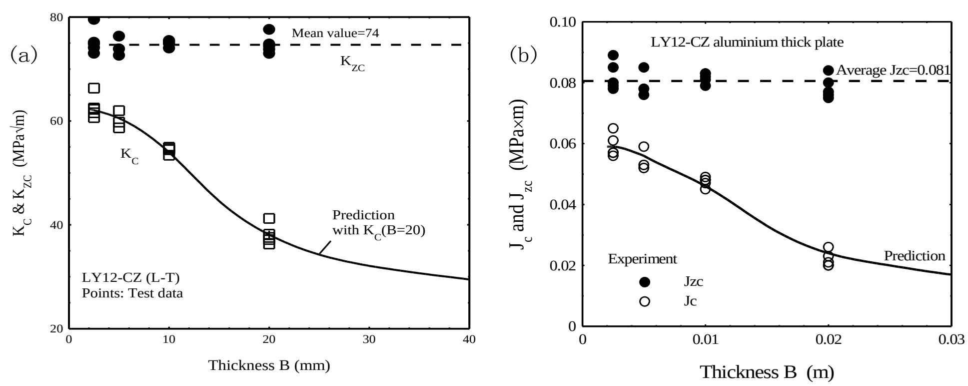

Fig. 3. Variation of two- and three- dimensional fracture toughness parameters K_C-K_{ZC} (a) and J_C-J_{ZC} (b) with thicknesses of test specimens.

4. 3D constraint effects on fatigue crack propagation

The famous Paris formula $da/dN=c(\Delta K)^m$ has been widely used in predicting the fatigue life of structures. Since plastic deformation near the crack tip is often unavoidable, it will cause a crack closure and reduce the effective range of SIF during a crack growth. In such a case the plasticity induced crack closure theory is used to describe the fatigue crack growth rate. Under small scale yielding, the $da/dN \sim \Delta K_{eff}$ curve can be expressed in the form of

$$\frac{\mathrm{d}a}{\mathrm{d}N} = F(\Delta K_{\mathrm{eff}}) \tag{10}$$

4.1 Crack closure model for through-thickness cracked bodies

For through-thickness cracked bodies, Chang and Guo [34] developed the range of ΔK_{eff} in Eq. (10) by combining the three-dimensional constraint theory [35] with the Budiansky–Hutchinson [36] model for crack closure, and gave an explicit expression of the ΔK_{eff}

$$\begin{aligned} &\Delta K_{\mathrm{eff}} = U\Delta K \\ &U = 1 - \frac{K_{\mathrm{open}}}{K_{\max}} = \eta^{1/3} \\ &\eta = (1-R^2)^2(1+10.34R^2)\times(1+1.67R^{1.61}+\frac{1}{0.15\pi^2\alpha_{\mathrm{g}}})^{-4.6} \end{aligned} , \tag{11}$$

where, R is the stress ratio, α_{g} is a combined constraint factor considering 3D stress status of the crack, and

$$\alpha_{\mathrm{g}} = \frac{1+0.208803(r_{\mathrm{p0}}/B)^{0.5}+1.0546(r_{\mathrm{p0}}/B)}{1-2v+0.208803(r_{\mathrm{p0}}/B)^{0.5}+1.0546(r_{\mathrm{p0}}/B)}, \tag{12}$$

where v is Poisson's ratio, $r_{\mathrm{p0}}=(\pi/8)(K_{\max}/\sigma_{\mathrm{flow}})^2$ is the Dugdale plastic zone radius, $\sigma_{\mathrm{flow}}=(\sigma_{0.2}+\sigma_{\mathrm{b}})/2$ is the flow stress of the material, B is the specimen thickness.

Eqs. (11) and (12) were used to evaluate ΔK_{eff} for through-thickness cracked bodies and the obtained da/dN~ΔK_{eff} curves are independent of stress ratio as well as the specimen thickness which was shown in Fig.4.[37]

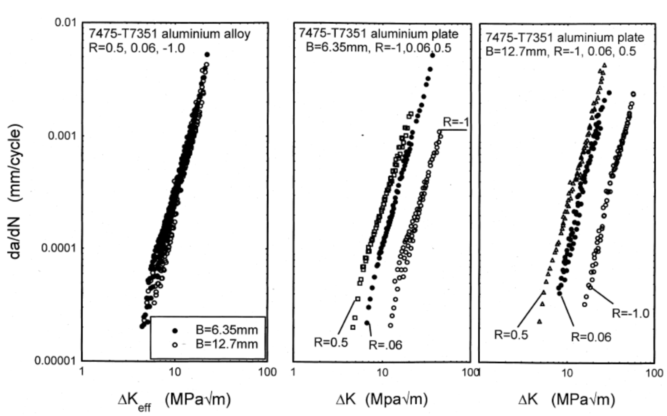

Fig. 4. Fatigue crack growth data in 7475-T7351 aluminum alloy: CCT specimens with different thicknesses.

4.2 Crack closure model for 3D cracked base on the concept of equivalent thickness B_{eq}

For through-thickness crack bodies, 3D plasticity induced crack closure effect for fatigue crack propagation can be evaluated by use of Eqs. (11) and (12). For 3D cracks bodies, however, the above Eqs. can not directly provide the local constraint factors α_{3D} along the crack tip line because of the difficulty in defining the thickness. So, a new concept of equivalent thickness B_{eq} was proposed [38] to replace the through-thickness B to calculate α_{3D}

$$\alpha_{3D} = \frac{1+0.208803(r_{p0}/B_{eq})^{0.5}+1.0546(r_{p0}/B_{eq})}{1-2\nu+0.208803(r_{p0}/B_{eq})^{0.5}+1.0546(r_{p0}/B_{eq})}, \tag{13}$$

The B_{eq} is defined as B_{eq}=2min{ B_1, B_2}. As shown in Fig.5, B_1 and B_2 are the distances from the analyzed point P at the crack front to the boundary of the cracked bodies along the tangential line of the crack front line at P. For elliptical surface crack in a round bar, the equivalent thickness B_{eq} at the deepest point P of crack is shown in Fig. 5 (a). Apparently the constraint factor α_{3D} on the 3D crack border is a function of the positions.

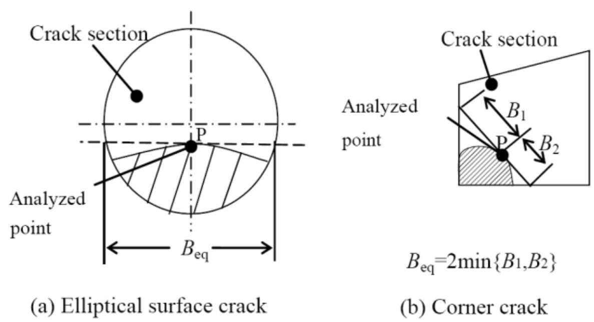

Fig.5. Definition of equivalent thickness B_{eq} for 3D cracked bodies.

A set of experimental da/dN~ΔK data[39, 40] for elliptical surface cracks round bars and standard through-thickness cracked specimens (with thickness of 15 mm and width of 30 mm) under constant amplitude loading (R=0.1 and 0.33) are presented in Fig.6 (a). But considering the crack closure effect the experimental points follow one curve as shown in Fig.6(b), obviously the three da/dN~ΔK curves are deviate from each other for different loading and geometry parameters. But on the condition that considering the crack closure effects, the da/dN~ΔK data in Fig. 6 (a) were analyzed using Eqs. (11)~(13) and the derived da/dN~ΔK_{eff} data appear in a unique curve which were shown in Fig.6 (b) [41]. Consequently, the 3D constraint effects on surface crack propagation were successfuly evaluated.

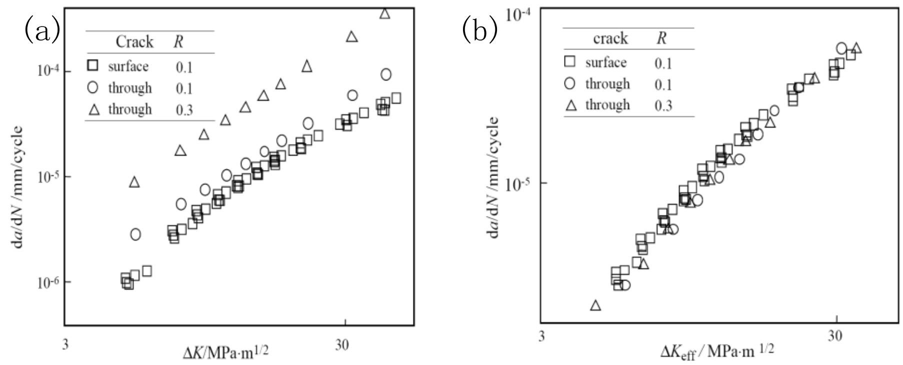

Fig.6 da/dN~ΔK (a) and da/dN~ΔK_{eff} (b) curves of 20CrMo steel.

By use of the latest achievements of constraint theory and the concept of equivalent thickness B_{eq}, 3D fatigue cracks propagation in complicated engineering structures can be analyzed effectively based on da/dN~ΔK curves of laboratory standard specimens.

5. Conclusion

The out-of-plane stress constraint factor T_z is a critical key parameter in the 3D fracture mechanics. The fracture and fatigue tests data from laboratory can be applied to the complex practical engineering structures in high rationality and efficiency.

References

[1] Irwin GR. Fracture, Handbuch der physic vol. VI, Flugge, (ed), Springer, 1958, 551-590.

[2] Williams ML. On the stress distribution at the base of a stationary crack. ASME J Appl Mech 1957, 24: 109~114.

[3] Rice JR. A path independent integral and approximate analysis of strain concentration by notches and cracks. J Appl Mech, 1968, 35: 379~386.

[4] Hutchinson JW. Singular behaviour at the end of a tensile crack in a hardening material. J. Mech. Phys. Solids, 1968, 16:13~31.

[5] Rice JR, Rosengren GF. Plane strain deformation near a crack tip in a power-law hardening material. J. Mech. Phys. Solids, 1968, 16: 1~12.

[6] Li Y, Wang Z. Higher order asymptotic field of tensile plane strain nonlinear crack problem. Scient Sin (Series A) 1986, 29: 941-255.

[7] Al-Ani AM, Hancock JW. J-dominance of short cracks in tension and bending. J Mech Phys Solids, 1991, 39:23~43.

[8] O'Dowd NP, Shih CF. Family of crack-tip fields characterized by a triaxiality parameter-II. Structure of fields. J. Mech. Phys. Solids., 1991, 39(8):989~1015.

[9] O'Dowd NP, Shih CF. Family of crack-tip fields characterized by a triaxiality parameter-I. Fracture application. J. Mech. Phys. Solids., 1992,40(8):939~963.

[10] Xia L, Wang TC, Shih CF. Higher-order analysis of crack tip fields in elastic power law hardening materials. J. mech. Phys. Solids, 1993, 41(4):665~687.

[11] Chao YJ, Yang S, Sutton MA. On the fracture of solids characterized by one or two parameters: theory and practice. J. Mech. Phys. Solids, 1994, 42(4):629~647.

[12] Andrzej Neimitz, Jaroslaw Galkiewicz. Fracture toughness of structural components: influence of constraint. Int. J. Pres. Ves. Pip. 2006; 83:42-54.

[13] Andrzej Neimitz, Modification of Dugdale model to include the work hardening and in- and out-of-plane constraints. Engng Fract Mech, 2004; 71:1585-1600.

[14] Andrzej Neimitz, Dugdale model modification due to the geometry induced plastic constraints. Engng Fract Mech, 2000; 67:251-261.

[15] Guo W. Elastoplastic three dimensional crack border field-I. Singular structure of the field. Engng Fract Mech, 1993, 46(1): 93~104.

[16] Guo W. Elastoplastic three dimensional crack border field-II. Asymptotic solution for the field. Engng Fract Mech, 1993, 46(1): 105~113.

[17] Guo W. Elasto-plastic three-dimensional crack border field-III. Fracture parameters. Engng Fract Mech, 1995, 51(1): 51~71.

[18] Guo WL. Recent advances in three-dimensional fracture mechanics. Key Eng. Mater. 2000, 183, 193-198.

[19] Junhua Zhao, Wanlin Guo, Chongmin She. The in-plane and out-of-plane stress constraint factors and K-T-T_z description of stress field near the border of a semi-elliptical surface crack. Int. J. Fatigue. 2007, 29: 435-443.

[20] J. Zhao, W. Guo and C. She. The three-parameter description of stress field near the border of an embedded elliptical crack. Acta Mechanica. 2007, 190: 29-44.

[21] Junhua Zhao, Wanlin Guo, Chongmin She, Bo Meng. Three dimensional K-T_z stress fields around the embedded center elliptical crack front in elastic plates. Acta Mechanica Sinica. 2006, 22 (2), 148-155.

[22] J. Zhao, W. Guo, C. She. The in-plane and out-of-plane stress constraint factors and K-T-T_z description of stress field near the border of a quarter-elliptical corner crack. Fatigue and Fracture of Engineering Materials and Structures. 2007, 30(8): 673-681.

[23] Junhua Zhao, Wanlin Guo and Chongmin She, Three-parameter approach for elastic-plastic fracture of the semi-elliptical surface crack under tension, Int. J. Mech. Sci. 2008, 50: 1168-1182.

[24] B Zhang, Three-dimensional fracture of macro-structures and failure of micro-materials. Nanjing, Nanjing University of Aeronautics and Astronautics, 2005.

[25] Bin Zhang, Wanlin Guo. T_z constraints of semi-elliptical surface cracks in elastic plates subjected to uniform tension loading. Int. J. Fracture. 2005, 131(2): 173~187.

[26] Irwin GR. Fracture mode transition for a crack traversing a plate. J. Basic Eng. 1960, 82: 417-425.

[27] Neimitz A, Galkiewicz J. Fracture toughness of structural components: influence of constraint. Int. J. Pres. Ves. Pip. 2006, 83: 42-54.

[28] Aoki S, Kishimoto K, Yoshida T, et al, Elastic-plastic fracture behavior of an aluminum alloy under mixed mode loading. J. Mech. Phys. Solids. 1990, 38; 195~213.

[29] Mills WJ, Hertzberg RW, The effect of thickness on fatigue crack retardation in 2024-T3 aluminum alloy. Eng. Fract. Mech. 1975, 7: 705~711

[30] Rigby RH, Aliabadi MH, Decomposition of the mixed-mode J-integral revised. Int. J. Solids Struct. 1998, 35: 2073~2099

[31] Guo W. 1991. Three dimensional fracture and fatigue crack propagation. Ph.D. dissertation, Northwestern Polytechnic University.

[32] Guo W L. Elastoplastic three-dimensional crack border II. Asymptotic solution for the field. Eng Fract Mech,1993,46 (1):105~113

[33] Junhua Zhao. Three-parameter research on three-dimensional fracture for macrostructures. Nanjing, Nanjing University of Aeronautics and Astronautics, 2008.

[34] Chang T, Guo W. A model for the through-thickness fatigue crack closure. Eng Fract Mech 1999; 64: 59-65.

[35] Guo W, Wang C, Rose F. The influence of cross-sectional thickness on fatigue crack growth. Fatigue Fract Engng Mater Struct .1999; 22: 437-444.

[36] Budiansky B, Hutchinson JW. Analysis of closure in fatigue crack growth. J Appl Mech. 1978; 45:267-276.

[37] Guo W. Three-dimensional analyses of plastic constraint for through-thickness cracked bodies. Eng Fracture Mech. 1999; 62: 383-407.

[38] Shen HJ, Guo W. 3D constraint effects on 3D fatigue crack propagation. Int J Fatigue, 2005; 27: 617-623.

[39] Keming Xu, Boming Z. Experimental study on stress intensity factors of tensile round bar with surface crack. Trans Daqing Petroleum College 1991; 15(2): 65-69 in Chinese.

[40] Guoli W, Jiaquan W. Probability analysis on crack propagation of sucker rod material. Trans Daqing Petroleum College 1993; 17(1): 78-83 in Chinese.

[41] Shen HJ, Guo W. 3D constraint effects on 3D fatigue crack propagation. Int J Fatigue. 2005; 27: 617-623.